Insights into increasing selenate reductase enzyme activity in the presence of nitrogen-doped graphite electrodes for selenium effluent treatment

Mohapatra, Dipti Prakash; Robinson, Kelly Ann; Huang, Fang; Kirpalani, Deepak; Loewen, Michele Christine

Publisher's version / Version de l'éditeur:
https://doi.org/10.3390/w14060931
Water, 14, 6, 2022-03-16

water

MDPI

Communication

Insights into Increasing Selenate Reductase Enzyme Activity in the Presence of Nitrogen-Doped Graphite Electrodes for Selenium Effluent Treatment

Dipti Prakash Mohapatra [1,*], Kelly Ann Robinson [2], Fang Huang [2], Deepak Kirpalani [1] and Michele Christine Loewen [2]

[1] Energy Mining and Environment Research Center, National Research Council of Canada, 1200 Montreal Road, Ottawa, ON K1A 0R6, Canada; deepak.kirpalani@nrc-cnrc.gc.ca
[2] Aquatic and Crop Resource Development Research Center, National Research Council of Canada, 100 Sussex Dr., Ottawa, ON K1A 0R6, Canada; kelly.robinson@nrc-cnrc.gc.ca (K.A.R.); fang.huang@nrc-cnrc.gc.ca (F.H.); michele.loewen@nrc-cnrc.gc.ca (M.C.L.)
* Correspondence: Dipti.Mohapatra@nrc-cnrc.gc.ca; Tel.: +1-613-993-9261

Abstract: The weathering of selenium-rich rocks or anthropogenic activities such as mining or smelting can release selenium into the environment, posing a significant environmental risk. The increased monitoring and enforcement of selenium regulations have resulted in protocols to efficiently measure and treat selenium in water and effluent water. The principal aqueous forms of inorganic selenium are selenite (Se(IV)) and selenate (Se(VI)). Selenate, due to its oxy-anionic nature, high mobility, and lack of affinity to conventional adsorbents, is typically more difficult to treat and remove. Thus, it is proposed to remove selenate from water by first reducing it to selenite and then to insoluble elemental selenium, a form that has low toxicity. A naturally occurring selenate reductase enzyme from *Thauera selenatis* was previously shown to specifically reduce selenate to selenite. To exploit this functionality, recombinant enzyme technologies were used to produce a cell-free, enriched *Thauera selenatis* selenate reductase heterotrimeric enzyme complex (*Ts*Ser-$\alpha\beta\gamma$). The addition of the recombinant enzyme complex to effluent water was found to successfully reduce the selenate. Interestingly, upon adding nitrogen-doped graphite electrodes to the reaction, the selenate-reducing activity significantly increased. Overall, these findings highlight a new, potentially sustainable solution to the reduction of selenate in water and effluent water.

Keywords: N2-doped graphite electrodes; effluent water; selenium; selenate reductase enzymes

check for updates

Citation: Mohapatra, D.P.; Robinson, K.A.; Huang, F.; Kirpalani, D.; Loewen, M.C. Insights into Increasing Selenate Reductase Enzyme Activity in the Presence of Nitrogen-Doped Graphite Electrodes for Selenium Effluent Treatment. *Water* **2022**, *14*, 931. https://doi.org/10.3390/w14060931

Academic Editor: Paola Verlicchi

Received: 27 January 2022
Accepted: 11 March 2022
Published: 16 March 2022

1. Introduction

Selenium, a ubiquitous element in mine water with high mobility and aqua toxicity, is a metalloid of significant concern that needs to be monitored and controlled. Industrial sources of selenium contamination in water sources include mine effluents, fossil fuel (coal and oil production), and precious metal refining. The development of low-cost, reliable technologies to remove selenium from effluent water is a priority for industry sectors, as the environmental standards and criteria applicable for their discharge must comply with new stringent discharge regulations. However, studies and the ensuing industrial implementation of microbial remediation in selenium reduction in small and large bioreactors have demonstrated the significant removal of selenium from effluent water by microbial remediation, where Se oxyanions (selenite (SeO_3^{2-}) and selenate (SeO_4^{2-})) are reduced to elemental selenium [1,2]. However, such a biological reduction yielded biogenic elemental Se nanoparticles (BioSeNPs) [1,3], requiring further treatment before discharging the effluent into the environment.

However, there have been some very significant technological developments over the last two decades in the area of industrial recombinant enzyme engineering and production,

including the optimization of purified enzyme yields, increased stability, and recoverability (immobilization) designs for applications in challenging environments [4–6]. Concurrently, there have been a number of reports highlighting the characteristics of naturally occurring enzymes with the potential to reduce selenate and selenite directly [7–13]. Additional reports have also demonstrated the reduction of selenite by reduced glutathione (a bio-based reducing agent) and the sequestration of the resulting elemental selenium into protein-based nanospheres [3]. Most notable is the discovery of a naturally occurring selenate reductase enzyme shown to specifically use selenate (with no affinity for competing nitrate molecules) as a terminal electron acceptor, reducing it to selenite [14,15]. In particular, the selenate reductase complex from *Thauera selenatis* (*Ts*Ser-αβγ) was purified from its native source and shown to be comprised of a heterotrimeric complex of α, β, and γ subunits roughly 96 kDa, 40 kDa, and 23 kDa in size, respectively, together eliciting selenate reduction [15]. The *Ts*Ser-αβγ complex uses a protein (cytochrome c4) as an electron donor for selenate reduction in vivo [11,16]. Interestingly, as highlighted previously for microbial selenite reduction and enzymatic nitrate reduction [17,18], the use of electrodes as electron donors for enzymatic-based selenate reduction reactions presents an intriguing line of inquiry.

The research described herein uses the knowledge gained regarding *Ts*Ser-αβγ combined with recent advances in recombinant enzyme techniques to produce purified, recombinant forms of each of the individual α, β, and γ subunits comprising the *Ts*Ser-αβγ enzyme complex. The reconstitution of the individual subunits into the heterotrimeric complex, achieved simply by mixing the purified subunits together, was validated by size exclusion chromatography. The obtained *Ts*Ser-αβγ complex was subsequently applied to selenate-containing samples of effluent water, confirming its ability to reduce selenate. Finally, the potential to use nitrogen-doped graphite electrodes as a source of electrons for the *Ts*Ser-αβγ reaction was confirmed, altogether setting the stage for the future development of a sustainable biocatalyst-based selenium remediation process.

2. Materials and methods

2.1. Chemicals and Materials

All chemicals were purchased from Millipore Sigma, unless otherwise indicated.

2.2. Recombinant Expression and Affinity Enrichment of TsSer-α, β, and γ Subunits

Optimized genes encoding each of the *Ts*Ser-αβγ subunits (based on amino acid sequences obtained from the NCBI protein database accession numbers CAB53372.1, CAB53373.1, and CAB53375.1 for the α, β, and γ subunits, respectively) were synthesized and cloned individually into the pEX-N-GST expression vector at the Sgf1 and Mut1restriction sites by Blue Heron Biotech (Bothwell, WA, USA). This yielded genes that encoded each subunit fused to an N-terminal Glutathione-S-Transferase (GST) tag. Each of the 3 obtained vectors was transformed individually into *E. coli* BL21 (DE3) cells. For protein production, LB media with 100 μg/mL ampicillin was inoculated and grown overnight at 37 °C and 180–200 rpm. The obtained overnight culture was used to inoculate (1:100 dilution) 500 mL of the same media and grown as described above to OD_{600} = 0.6–0.7, at which point the temperature was reduced to 18 °C. Then the cultures were induced with 0.3 mM isopropyl β-D-1-thiogalactopyranoside and incubated overnight for 18 h. The cell cultures were harvested by centrifugation at 3270× *g* for 20 min at 4 °C, and the cell pellets were stored at −20 °C.

For protein purification, the cell pellets were thawed on ice and re-suspended in 20 mL of lysis buffer (PBS-L; 1X phosphate-buffered saline (PBS), pH 7.2, 1 mM dithiothreitol (DTT; Gold Bio, St. Louis, MO, USA), 1 mM ethylenediaminetetraacetic acid (EDTA), 1% Triton X−100) with lysis enzymes and protease inhibitors (0.1 mM phenylmethylsulfohyl fluoride (Gold Bio), 3 U/mL benzonase, 1 mg/mL lysozyme (Gold Bio) and incubated end-over-end at 4 °C for 30 min. The suspension was filtered through cheesecloth and lysed using an Emulsiflex C5 homogenizer (Avestin Inc., Ottawa, ON, Canada). The obtained

lysates were centrifuged at 15,000× *g* for 30 min at 4 °C, and the resulting supernatants were batch loaded onto Glutathione HiCap Matrix columns (QIAGEN, Valencia, CA, USA), pre-equilibrated in 10 column volumes (CV) of equilibration buffer (1X phosphate-buffered saline (PBS), pH 7.2, 1 mM DTT, and 1 mM EDTA), and incubated for 30 min at 4 °C. The loaded columns were washed twice with 5 CV of equilibration buffer each time. The GST-tagged recombinant subunits were eluted using 4 × 1.5 mL elution buffer (50 mM Tris-HCl, pH 8.0, 0.4 M NaCl, 0.1% Triton X-100, 1 mM DTT, and 50 mM reduced L-glutathione). Eluted fractions were collected at 4 °C, pooled, and concentrated to 500 µL using Corning® Spin-X® UF Concentrators (6 mL, 30 kDa MWCO) at 4 °C, followed by buffer exchange to 50 mM NaH_2PO_4, pH 7.2, 300 mM NaCl buffer. The purified recombinant proteins were quantified using the Bradford protein assay [19].

2.3. Validation of *Ts*Ser-αβγ Heterotrimeric Complex Formation

Recombinantly produced *Ts*Ser-α, -β, and -γ subunits were pooled in a 1:1:1 protein ratio with a final concentration of approximately 1 mg/mL total protein, and applied to a 120 mL HiLoad™ 16/60 Superdex200 prep grade column (GE Healthcare Life Sciences, Chicago, IL, USA) pre-equilibrated with gel filtration buffer (50 mM NaH_2PO_4 pH 7.2, 300 mM NaCl) using an AKTA Fast Performance Liquid Chromatography (FPLC) system (Amersham Biosciences; Poway, CA, USA) with UNICORN™ 4.0 software (Cytiva, Marlborough, MA, USA) at a flow rate of 1 mL/min using ice-cold buffer. The fractions were collected in 1.5 mL volumes on ice. The elution times were compared to the gel filtration protein standards (#151-1901, Bio-Rad, Mississauga, ON, Canada) that were run separately to estimate molecular weights.

The samples eluted from the size exclusion column were analyzed by 12% Tris-HCl sodium dodecyl sulfate-polyacrylamide gel electrophoresis (SDS-PAGE) with Precision Plus Protein Unstained Standards (Bio-Rad, Mississauga, ON, Canada) and/or Colour Protein Standard (10–250 kDa, New England Biolabs, Whitby, ON, Canada). The gels were stained using Coomassie Brilliant Blue or analyzed by Western blot analysis. For Western blot analysis, the gels were transferred to polyvinylidene difluoride (PVDF; Bio-Rad) membranes (pre-soaked in 100% methanol) using 1X transfer buffer (25 mM Tris, 190 mM glycine, 0.05% SDS, 20% methanol) for 90 min at 100 V on ice. The PVDF membranes were rinsed with distilled water and blocked in 5% skim milk in 1 X Tris-buffered saline with Tween-20 (TBST; 20 mM Tris-HCl, 150 mM NaCl, 0.12% Tween-20, pH 7.6) overnight at 4 °C with shaking. The blocked membranes were incubated for 1 h with shaking with Anti-GST mouse mAb (Origene, TA150101, Burlington, ON, Canada) at a 1:4000 dilution, washed with 1X TBST, and then incubated for 1 h with both 1:1000 diluted peroxidase-conjugated Goat anti-mouse IgG (TA130003, Origene) and 1:7500 diluted Precision Protein Strep Tactin-HRP conjugate (Bio-Rad #1610380, Mississauga, ON, Canada), the latter to visualize the protein standards. The blot was developed using Supersignal West Dura Extended Duration Substrate (Fisher Thermo Scientific. Waltham, MA, USA). Images were obtained using the ChemiDoc™ MP Imaging System (Bio-Rad) and ImageLab 5.2.1.

2.4. Selenate Reduction by the *Ts*Ser-αβγ Heterotrimeric Complex

Samples of the recombinant, enriched *Ts*Ser-αβγ reductase complex were produced by mixing the individual subunit samples together at 1:1:1 and 4:1:4 subunit ratios and at a final concentration of approximately 1 mg/mL protein in each sample. The ability of these reconstituted *Ts*Ser-αβγ reductase complex mixtures to reduce selenate was evaluated by adding 10 µL of the enzyme sample to 200 mL of selenate-containing mining effluent water. Parallel experiments with control samples of Milli-Q water containing 10 ppm selenate were also conducted. The reactions were incubated at room temperature with shaking at 200 rpm for 1 h and subsequently analyzed for total selenium by inductively coupled plasma mass spectrometry (ICP-MS). The experiment was repeated 3 times. The initial and final concentrations of selenium after treatment were measured by ICP-MS in order to establish the efficiency of the enzymatic treatment process.

Subsequently, the effect of the presence of nitrogen-doped graphite electrodes, set up as presented in Figure 1, was assessed. The experiments were carried out in 200 mL Milli-Q water with 10 ppm selenate and adding 10 µL of the 1:1:1 *Ts*Ser-αβγ complex. The solutions were continuously stirred, and the samples were collected every 15 min for analysis of the selenium concentration as described above. The experiments were carried out at a power input of 15 V, 0.04 A. Nitrogen-doped graphite electrodes were applied due to their inherent benefits, including high resistance to corrosion in mine water (acidic). However, the electrodes are subject to oxidation and loss of carbon during operations at higher voltages (>1.26 V). The electrodes were prepared by treating graphite electrodes with a 25% ammonia solution at 180 °C for 4 h in an oven to increase the number of polar nitrogenous groups on the graphite surface to improve the electrochemical activity of the electrodes and reduce the potential for nitrate accumulation on the anode. The electrodes were washed with deionized water until a neutral pH was reached in the rinse water. The electrodes were dried at 110 °C in an oven for 24 h.

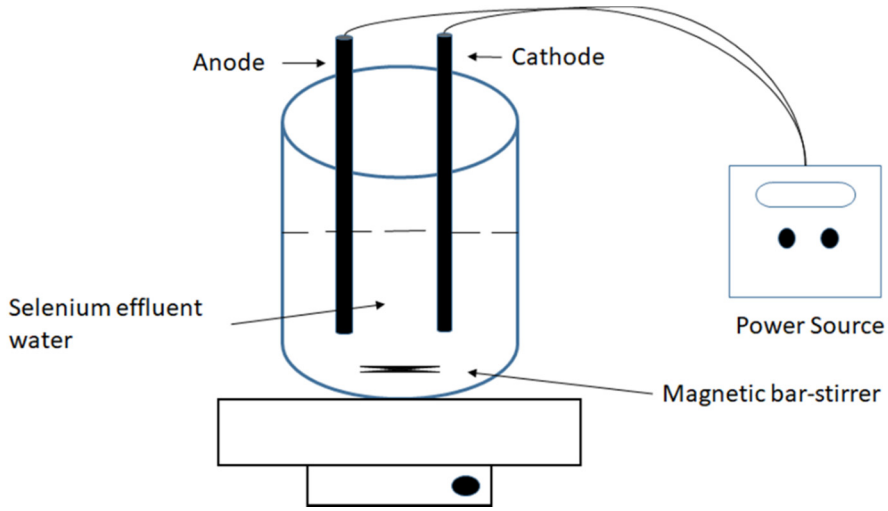

Figure 1. Experimental set-up for selenium reduction from effluent water in the presence of carbon electrodes and the *Ts*Ser-αβγ enzyme complex.

3. Results and Discussion

3.1. Expression and Purification of the Individual TsSer-α, -β, and -γ Subunits

Initially, the ability to recombinantly produce and purify the three target *Ts*Ser-α, -β, and -γ subunits was assessed. Following the transformation of the expression constructs encoding the GST-fused subunit proteins into *E. coli* BL21 (DE3) cells, protein production was induced, the obtained cell pellets were lysed, and the target proteins were individually purified by GST-affinity chromatography. The eluted protein samples were visually assessed by Coomassie-stained SDS-PAGE (Figure 2). The background bands in all the samples emphasized that the GST-fusion proteins were not purified to complete homogeneity by this one-step enrichment. Nonetheless, the sample containing the GST-*Ts*Ser-β fusion protein yielded a significantly overloaded band at ~60 kDa, consistent with its expected Mw of 66 kDa. While not as pronounced, the GST-*Ts*Ser-γ fusion protein sample yielded a prominent band, not detected in any of the other samples, at ~50 kDa, consistent with its expected Mw of 49 kDa. In this case, a significant band was also detected at ~26 kDa, as well as another band of equivalent intensity at ~23 kDa, consistent with the possibility that the bulk of the GST-*Ts*Ser-γ fusion protein was proteolytically released into its primary components of GST (expected Mw 26 kDa) and *Ts*Ser-γ (expected Mw 23 kDa) after elution from the column. Finally, the sample containing the GST-*Ts*Ser-α fusion protein yielded a visible band at ~130 kDa, which was not present in any of the other sample sand approximately consistent with its expected Mw of 122 kDa.

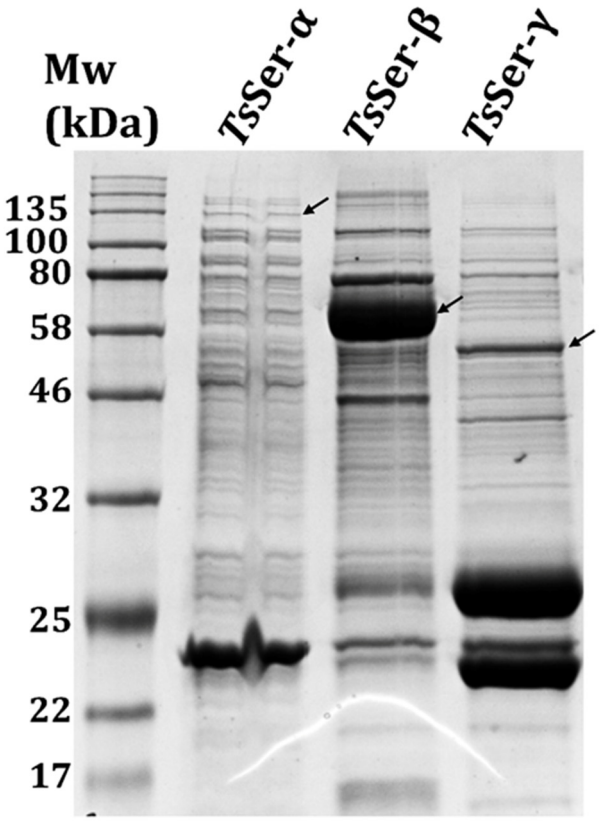

Figure 2. Enrichment of recombinantly produced individual GST-tagged *Ts*Ser-α, -β, and -γ subunits. Cells expressing the individual subunits were lysed and the obtained soluble fractions applied to GST-affinity chromatography. The eluted enriched protein fractions were visualized by SDS-PAGE analysis, with Coomassie Brilliant Blue staining. Black arrows indicate the expected positions of bands for each GST-tagged *Ts*Ser-α, -β, or -γ subunit.

3.2. Validation Heterotrimeric TsSer-αβγ Complex Formation

The individual subunits were not expected to have any enzymatic activity on their own. In order to reconstitute the active heterotrimeric *Ts*Ser-αβγ complex, the three purified subunit samples were mixed together at a 1:1:1 ratio of total protein detected in each sample, and at a final concentration of 1 mg/mL total protein. Following a brief incubation, the mixture was applied to a size exclusion column in an attempt to detect the formation of the heterotrimeric complex. Examination of the elution profile highlights three major peaks at 41, 44 (shoulder), and 78–80 min, respectively (Figure 3A). The calibration of the column suggests that the heterotrimeric *Ts*Ser-αβγ complex (expected Mw ~250 kDa with GST-tags) should elute at ~50 min. The individual (non-complexed) subunits are expected to elute later, at 70 min (α; 120 kDa) and 85 min (β and γ; 66 kDa and 49 kDa), respectively. The collected peak fractions were pooled, concentrated, and analyzed by Coomassie stain SDS-PAGE (Figure 3B). While very little protein was detected in the 41 min fraction, the 44 min fraction yielded an array of bands, including those at the expected molecular weights for all three of the GST-subunit fusion proteins as well as *Ts*Ser-α and *Ts*Ser-γ, both in their unfused forms. The identities of the GST-subunit fusion proteins were subsequently confirmed by Western blot analysis using anti-GST antibody (Figure 3C), clearly revealing the presence of all 3 expected GST-fusion subunits in the 44 min fraction. The fact that the 23 kDa band was detected by the anti-GST Ab in both the 44 and 78 min fractions suggests it may be a truncated form of GST, if not a mixture of truncated GST with free *Ts*Ser-γ. Nonetheless, the 44 min elution fraction was within 6 min of the expected elution time (50 min) for the heterotrimeric complex, and more than 25 min ahead of the expected elution of even the biggest monomeric subunit, emphasizing the successful

trimeric complex formation. Whether the 6 min shift represents variability in the calibration or a genuinely larger oligomeric state (44 min could potentially be consistent with a 500 kDa dimer of the trimer) remains for future evaluation.

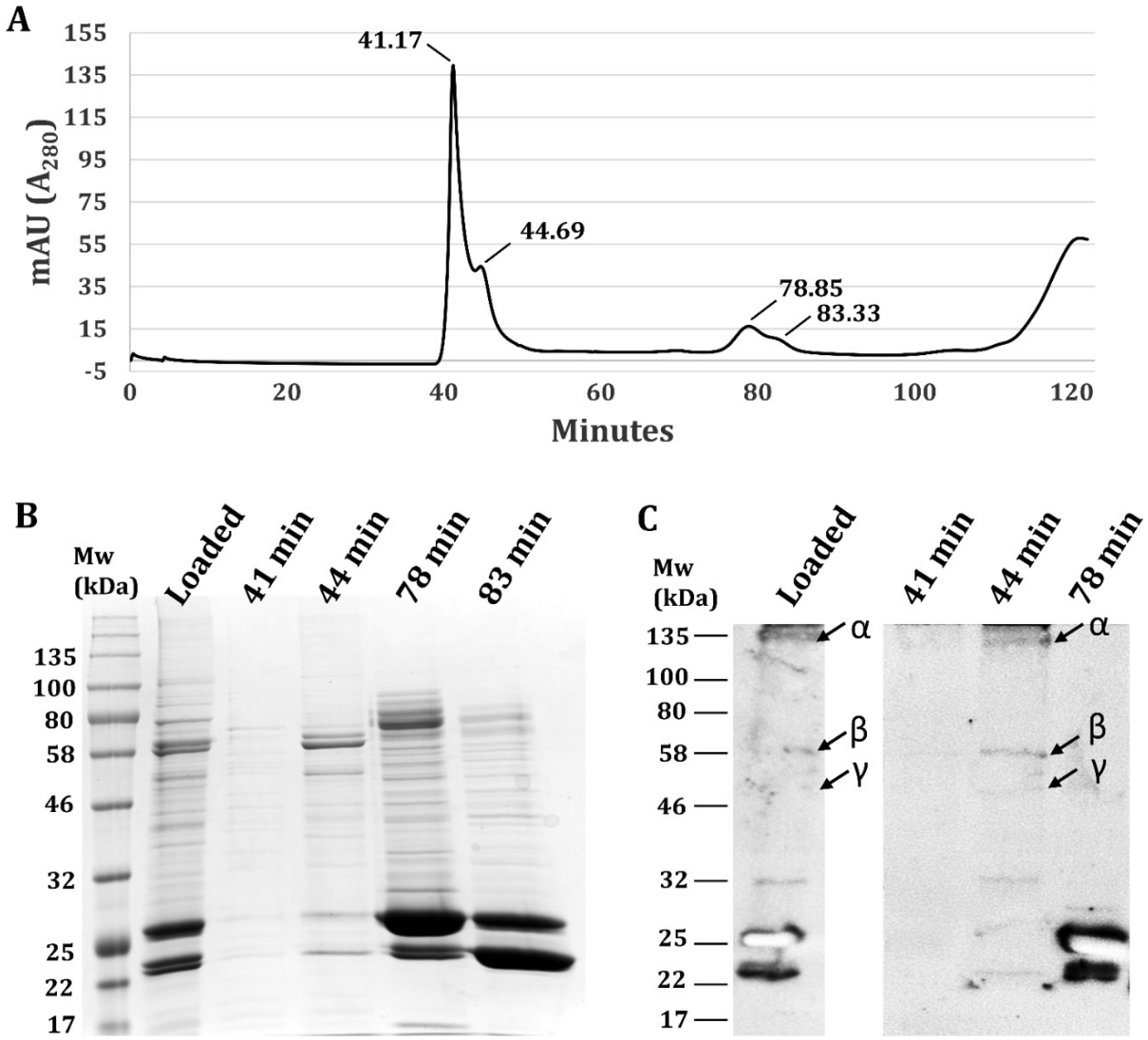

Figure 3. Validation of *Ts*Ser-αβγ heterotrimer formation. (**A**) Size exclusion chromatography profile. The affinity-enriched GST-tagged subunits were mixed together to allow for heterotrimeric complex formation, and then analyzed by size exclusion chromatography using a HiLoad™ 16/60 Superdex200pg. Peaks are labelled with elution times. Eluted fractions representing the main peaks (as indicated by the times) were analyzed by (**B**) SDS-PAGE stained with Coomassie Brilliant Blue or (**C**) Western blot probed with Anti-GST antibody. The 'Loaded' lane is the mixture of all three subunits prior to size exclusion separation. Black arrows indicate the expected positions of bands for each GST-tagged *Ts*Ser-α, -β, or -γ subunit.

3.3. Enzymatic Reduction of Selenium by Recombinantly Produced TsSer-αβγ Enzyme Complex from Effluent Water

Enzymatic selenium reduction studies using the recombinantly-produced *Ts*Ser-αβγ complex described above were carried out in Milli-Q water in the presence and absence of selenium as well as in real mining effluent water samples. The *Ts*Ser-αβγ complex was prepared by mixing aliquots of the individual purified subunit samples at both 1:1:1 and 4:1:4 ratios (by volume) for the α, β, and γ subunits, respectively; the latter ratio was to account for differences in the yields of the individual subunits. Following the addition

of the *Ts*Ser-αβγ complex mixtures to selenate-containing (10 ppm) Milli-Q water, the selenium levels were reduced by 26% (±2) and 21% (±1.5) for the 1:1:1 and 4:1:4 ratios, respectively, compared to the untreated controls. In the mining effluent water, the selenium levels were also reduced, albeit less efficiently, by 19% (±1.2) and 14% (±1.8) for the *Ts*Ser-αβγ complexes at the 1:1:1 and 4:1:4 ratios, respectively, compared to the untreated controls. The selenate reductase enzyme complex included iron, molybdenum, and acid-labile sulfur co-factors that contributed to the electronic mechanism underlying its ability to reduce selenate.

Subsequently, the effect of providing a source of electrons on the enzymatic activity of the *Ts*Ser-αβγ complex was evaluated. Experiments were carried out with the addition of nitrogen-doped graphite electrodes in the presence or absence (negative control) of the *Ts*Ser-αβγ complex formed at a 1:1:1 ratio of the subunits. The experiment was conducted in Milli-Q water with a spiked selenate concentration of 10 ppm (Figure 1). The levels of selenium were found to be significantly reduced (61%) in the presence of electrodes with the *Ts*Ser-αβγ complex as compared to the control sample (24%) (Figure 4). Furthermore, these results demonstrate that in the presence of electrodes, the activity of the enzymes was increased, yielding higher selenium removal from the medium.

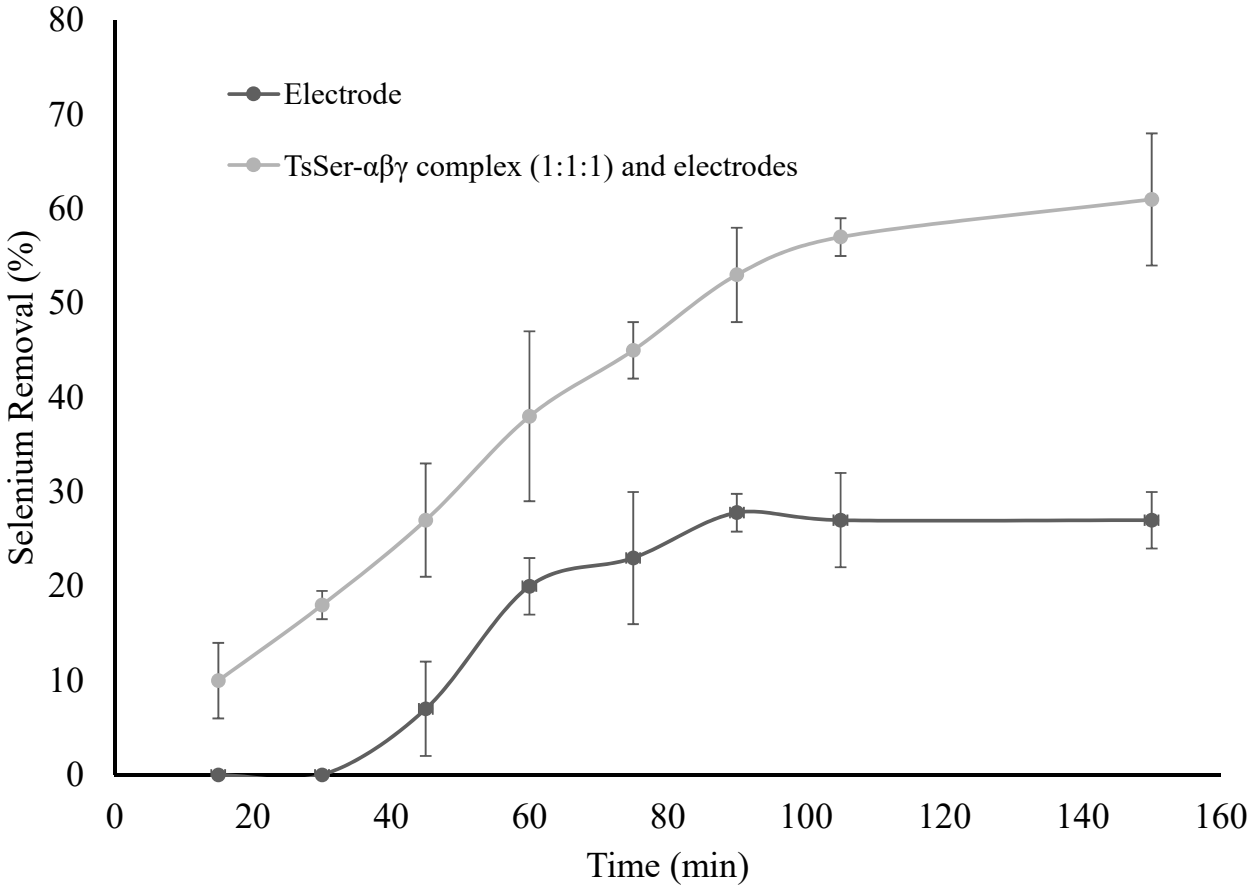

Figure 4. Selenium reduction from effluent water with carbon electrodes in the presence and absence of the *Ts*Ser-αβγ complex.

4. Conclusions

A recombinantly produced functional *Ts*Ser-αβγ complex was shown to be formed with demonstrated activity against the water samples containing selenate. This was achieved by taking advantage of the very significant technological developments over the last two decades in the area of industrial recombinant enzyme production for enhanced yield, enrichment, and complex recombination. Furthermore, the demonstrated benefits of providing a source of electrons to the biocatalyst through the inclusion of nitrogen-doped

graphite electrodes in the reaction further emphasize the potential of this technology to lead to a sustainable solution for the reduction of selenate from mining effluent water and other industrial sources. Future efforts will focus on the optimization of the biocatalyst stability and efficiency, as well as testing the benefits of immobilization and recoverability.

Author Contributions: Conceptualization, D.P.M. and M.C.L.: methodology, D.P.M. and M.C.L.; experimental and results interpretation, D.P.M., K.A.R., F.H. and M.C.L.; original draft preparation, D.P.M., K.A.R. and M.C.L.; Review and editing, D.K. All authors have read and agreed to the published version of the manuscript.

Funding: This research received no external funding.

Data Availability Statement: Not applicable.

Acknowledgments: The authors would like to acknowledge the support provided by the National Research Council of Canada's Environmental Advances in Mining (EAM) Program.

Conflicts of Interest: The authors declare no conflict of interest.

References

1. Martínez, F.G.; Moreno-Martin, G.; Pescuma, M.; Madrid-Albarrán, Y.; Mozzi, F. Biotransformation of selenium by lactic acid bacteria: Formation of seleno-nanoparticles and seleno-amino acids. *Front. Bioeng. Biotechnol.* **2020**, *8*, 506. [CrossRef] [PubMed]
2. Sabuda, M.C.; Rosenfeld, C.E.; DeJournett, T.D.; Schroeder, K.; Wuolo-Journey, K.; Santelli, C.M. Fungal Bioremediation of selenium-contaminated industrial and municipal wastewaters. *Front. Microbiol.* **2020**, *11*, 2105. [CrossRef] [PubMed]
3. Debieux, C.M.; Dridge, E.J.; Mueller, C.M.; Splatt, P.; Paszkiewicz, K.; Knight, I.; Florance, H.; Love, J.; Titball, R.W.; Lewis, R.J.; et al. A bacterial process for selenium nanosphere assembly. *Proc. Natl. Acad. Sci. USA* **2011**, *108*, 13480–13485. [CrossRef] [PubMed]
4. Liu, L.; Yang, H.; Shin, H.D.; Chen, R.R.; Li, J.; Du, G.; Chen, J. How to achieve high-level expression of microbial enzymes: Strategies and perspectives. *Bioengineered* **2013**, *4*, 212–223. [CrossRef] [PubMed]
5. Rehm, F.B.H.; Chen, S.; Rehm, B.H.A. Enzyme engineering for in situ immobilization. *Molecules* **2016**, *21*, 1370. [CrossRef] [PubMed]
6. Singh, R.K.; Tiwari, M.K.; Singh, R.; Lee, J.K. From protein engineering to immobilization: Promising strategies for the upgrade of industrial enzymes. *Int. J. Mol. Sci.* **2013**, *14*, 1232–1277. [CrossRef] [PubMed]
7. Connelly, K.R.S.; Stevenson, C.; Kneuper, H.; Sargent, F. Biosynthesis of selenate reductase in *Salmonella enterica*: Critical roles for the signal peptide and DmsD. *Microbiology* **2016**, *162*, 2136–2146. [CrossRef] [PubMed]
8. Wells, M.; McGarry, J.; Gaye, M.M.; Basu, P.; Oremland, R.S.; Stolz, J.F. Respiratory selenite reductase from *Bacillus selenitireducens* strain MLS10. *J. Bacteriol.* **2019**, *201*, e00614–e00618. [CrossRef] [PubMed]
9. Yanke, L.; Bryant, R.; Laishley, E. Hydrogenase I of *Clostridium pasteurianum* functions as a novel selenite reductase. *Anaerobe* **1995**, *1*, 61–67. [CrossRef]
10. Maher, M.J.; Macy, J.M. Biological Crystallography Crystallization and preliminary X-ray analysis of the selenate reductase from *Thauera selenatis*. *Acta Crystallogr. Sect. D Biol. Crystallogr.* **2002**, *58*, 706–708. [CrossRef] [PubMed]
11. Kuroda, M.; Yamashita, M.; Miwa, E.; Imao, K.; Fujimoto, N.; Ono, H.; Nagano, K.; Sei, K.; Ike, M. Molecular cloning and characterization of the srdBCA operon, encoding the respiratory selenate reductase complex, from the selenate-reducing *Bacterium Bacillus selenatarsenatis* SF-1. *J. Bacteriol.* **2011**, *193*, 2141–2148. [CrossRef] [PubMed]
12. Guymer, D.; Maillard, J.; Sargent, F. A genetic analysis of in vivo selenate reduction by Salmonella enterica serovar Typhimurium LT2 and Escherichia coli K12. *Arch. Microbiol.* **2009**, *191*, 519–528. [CrossRef] [PubMed]
13. Yee, N.; Choi, J.; Porter, A.W.; Carey, S.; Rauschenbach, I.; Harel, A. Selenate reductase activity in *Escherichia coli* requires Isc iron-sulfur cluster biosynthesis genes, FEMS. *Microbiol. Lett.* **2014**, *361*, 138–143. [CrossRef] [PubMed]
14. Recht, S.A.; Macy, A.J.M. The terminal reductases for selenate and nitrate respiration in *Thauera selenatis* are two distinct enzymes. *J. Bacteriol.* **1992**, *174*, 7316–7320. [CrossRef] [PubMed]
15. Schröder, I.; Rech, S.; Krafft, T.; Macy, J.M. Purification and characterization of the selenate reductase from *Thauera selenatis*. *J. Biol. Chem.* **1997**, *272*, 23765–23768. [CrossRef] [PubMed]
16. Krafft, T.; Bowen, A.; Theis, F. Cloning and sequencing of the genes encoding the periplasmic-cytochrome B-containing selenate reductase of *Thauera selenatis*. *DNA Seq.* **2000**, *10*, 365–377. [CrossRef] [PubMed]
17. Nguyen, V.K.; Park, Y.; Yu, J.; Lee, T. Microbial selenite reduction with organic carbon and electrode as sole electron donor by a bacterium isolated from domestic wastewater. *Bioresour. Technol.* **2016**, *212*, 182–189. [CrossRef] [PubMed]

18. Gates, A.J.; Marritt, S.J.; Bradley, J.M.; Shi, L.; McMillan, D.G.; Jeuken, L.J.; Richardson, D.J.; Butt, J.N. Electrode assemblies composed of redox cascades from microbial respiratory electron transfer chains. *Biochem. Soc. Trans.* **2013**, *41*, 1249–1253. [CrossRef] [PubMed]
19. Bradford, M.M. A rapid and sensitive method for the quantitation of microgram quantities of protein utilizing the principle of protein-dye binding. *Anal. Biochem.* **1976**, *72*, 248–254. [CrossRef]